MAPPING HAWAIIAN LAVA FLOWS WITH *ECOSTRESS* AND *ASTER* TIR DATA

Michael Abrams
Jet Propulsion Laboratory, California Institute of Technology
Pasadena, CA

Introduction

The June, 2018 launch of ECOSTRESS to the International Space Station provided a second spaceborne, high spatial resolution multispectral thermal infrared imager, in addition to NASA's 19-year old ASTER instrument on the Terra spacecraft. While ECOSTRESS has similar spectral bands to ASTER (***Figure 1***), and a similar FOV, it benefits from an almost 400 kilometer wide swath, compared to ASTER's 60 kilometer swath (***Table 1***). ECOSTRESS' primary mission is to measure plant temperature to understand water need and response to stress. Nevertheless, the data can also be used for geologic applications, including mapping of volcanic lava flows. The Mauna Loa volcano on the Island of Hawaii provides an ideal test site to compare the capability of both instruments. Lava flows at higher elevations are vegetation-free, there are numerous pahoehoe and a'a flows with a wide range of eruption ages, and an excellent map exists for the area (***Figure 3***).

	ECOSTRESS	ASTER
# TIR Bands	5	5
Spectral range	8.3-12.1 µm	8.2-11.3 µm
FOV	50 degrees	8 degrees
Pixel size	69 x 38 m	90 m
Swath	384 km	60 km

Table 1. Characteristics of ECOSTRESS on the ISS and ASTER on Terra.

Spectral Response Functions

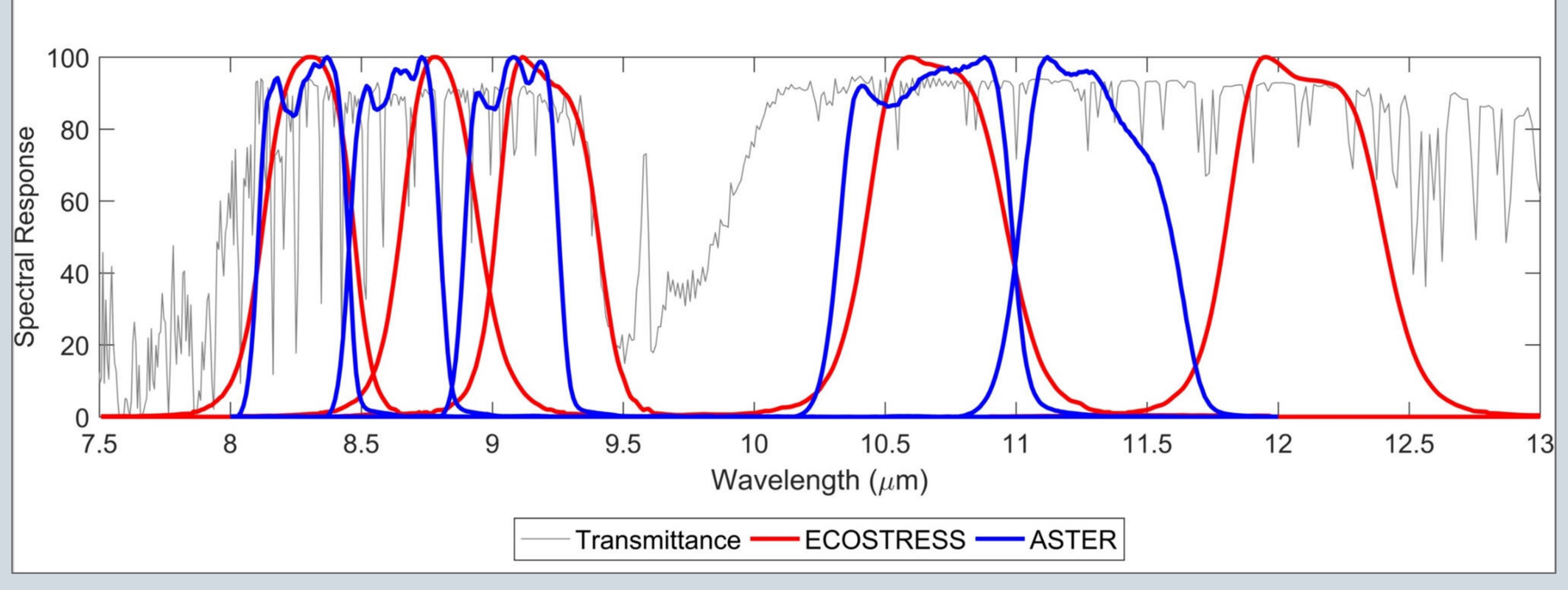

Fig. 1. Spectral response functions of ECOSTRESS (red) and ASTER (blue). ECOSTRESS band 5 (12.1 µm) was chosen to match MODIS Band 12, rather than ASTER band 14 (courtesy of Glynn Hulley, JPL).

Background

We analyzed the flows on the east flank of Mauna Loa volcano, imaged by the ASTER and ECOSTRESS TIR scanners. The basalt flows extend eastward, and some reach the sea and underlie Hilo. Flows range in age from the 20th century (red), to 10-15,000 years BP (blue), and are of both pahoehoe (thin, ropy flows) and a'a (blocky, clinker, thick flows) types (***Figure 3).*** The oldest flows are completely vegetated, and recent flows are completely free of vegetation.

Laboratory spectra in the 7-14 µm wavelength region of Hawaiian basalts (***Figure 2***), exhibit six features, both broadband and sharp. As weathering progresses, feature *b* becomes dominant. Subsequently, feature *a* appears as a shoulder on *b*. Finally, as weathering progresses, surfaces become coated with iron oxides and spectral contrast disappears. Feature *b* is due to development of sheet structures in the glass rind and decreases due to physical spalling. Shoulder *a* is due to an amorphous silica coating (cryptocrystalline quartz) that develops with further weathering. Feature *e* is due to hydration and development of silica rinds with further age (Abbott et al., 2013, Crisp et al., 1990, Farr and Adams, 1984).

TIR mapping of Hawaiian lava flows was initiated by our early work using the airborne Thermal Infrared Multispectral Scanner (TIMS) (Kahle et al., 1988, and Abrams et al., 1990). ASTER's TIR bands, and ultimately, ECOSTRESS' TIR bands, were modeled after the TIMS bands that proved so successful in numerous and varied campaigns. The placement of the bands covered the silicate Reststrahlen region, and emphasized silica content of rocks.

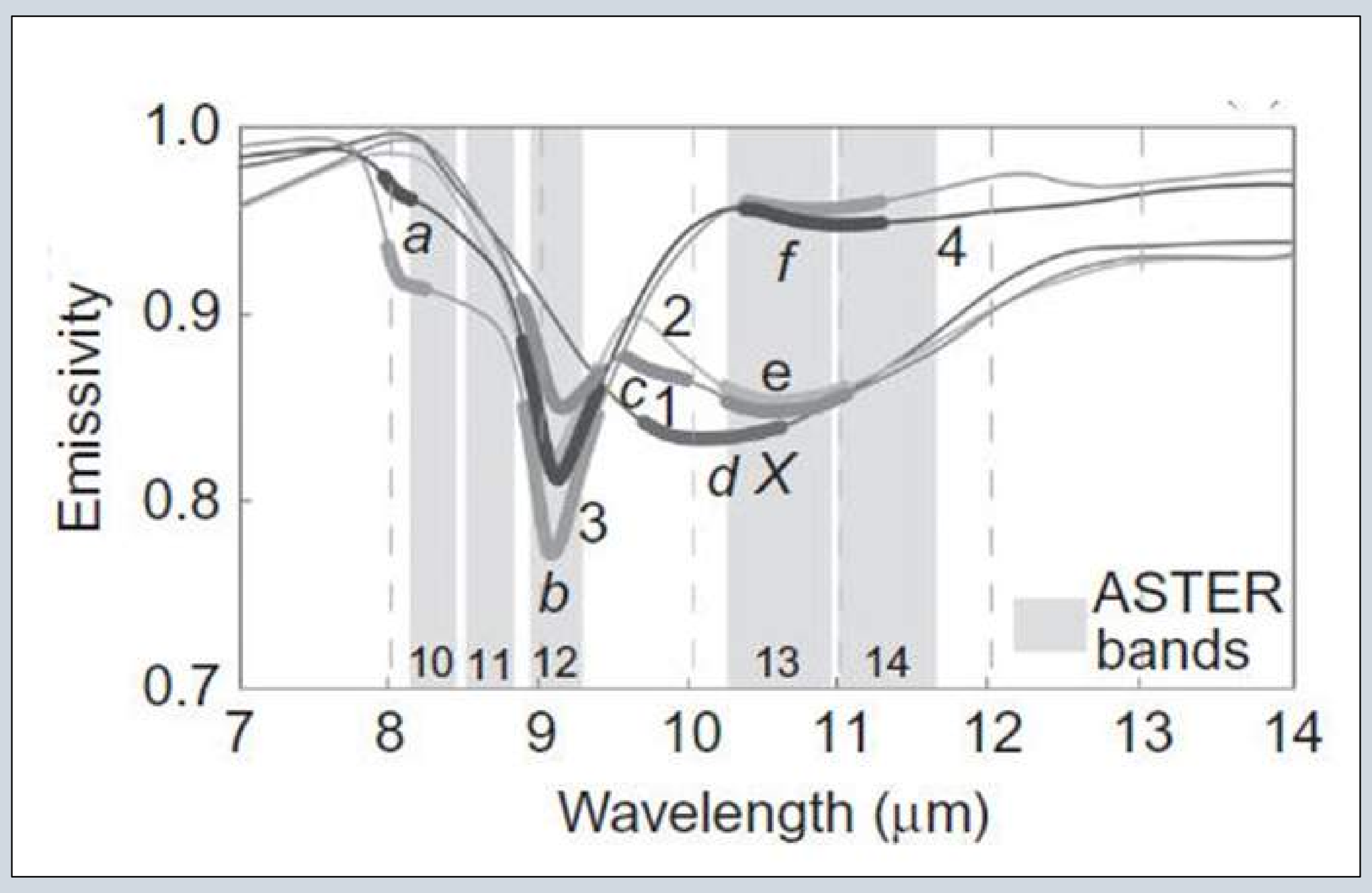

Fig. 2. Laboratory emissivity spectra of Mauna Loa basalts (Abbott et al., 2013)

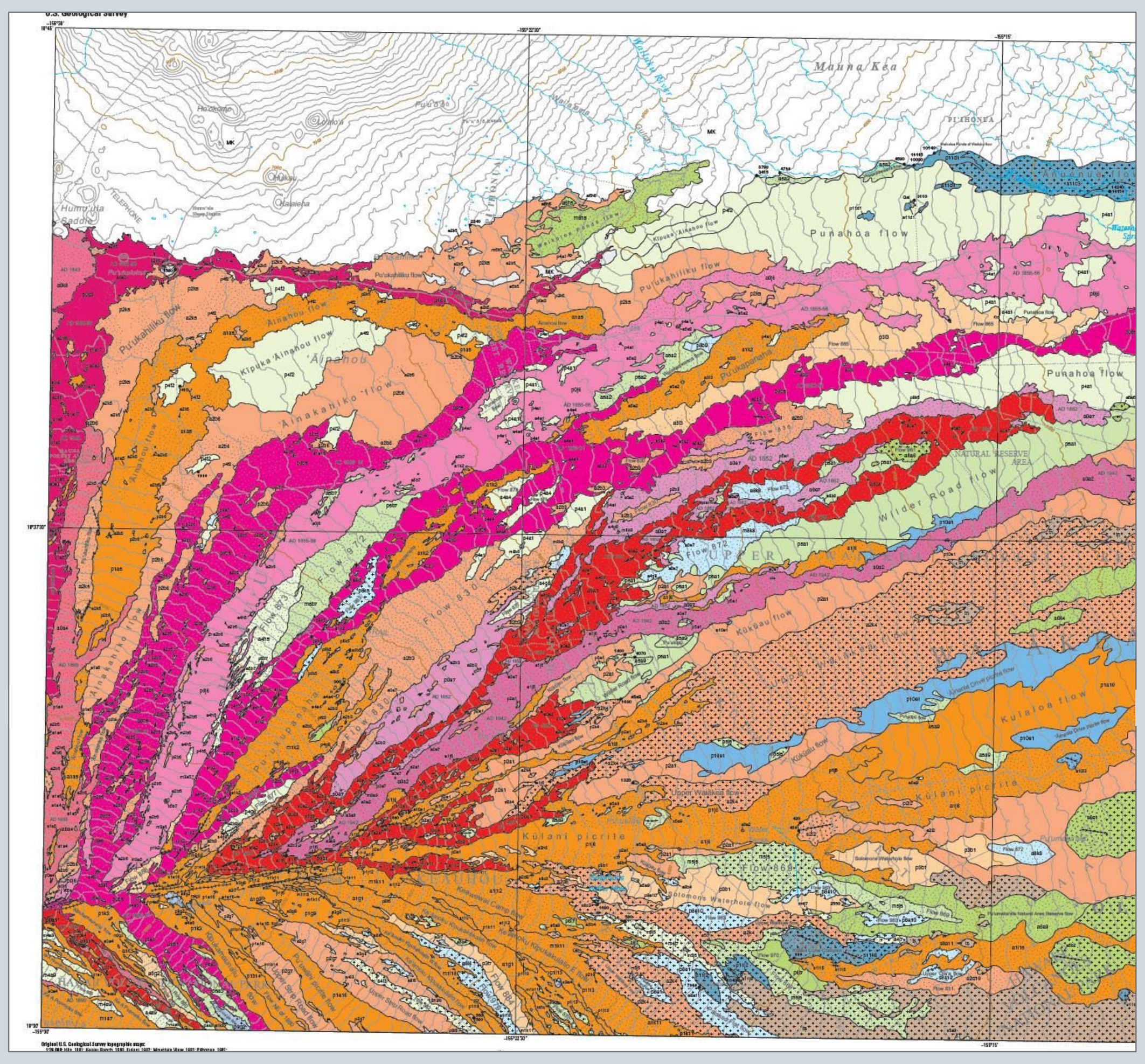

Fig 3. Geologic map of NE flank of Mauna Loa (Trusdell and Lockwood, 2017). Map covers 28.6 by 31 km.

Discussion

We have analyzed both daytime and nighttime images from ECOSTRESS and ASTER. Since the lava surfaces do not evince any seasonal variation, selection of images was based on minimizing cloud cover. ASTER images were acquired November 2, 2017 (day) and June 22, 2017 (night). ECOSTRESS data were acquired September 2, 2018 (night). No clear daytime images were acquired. Bands 1-4 from ECOSTRESS and bands 10-13 from ASTER were used. Following the early TIMS work (Kahle et al., 1988) we displayed ASTER bands 13-12-10 in RGB, and applied a decorrelation stretch (***Figure 4*** nighttime, ***Figure 5*** daytime). Referring to the map, we find there is a pronounced and systematic color change with age of pahoehoe: the color shifts from blue to purple and magenta. Young a'a are dark blue, and this shifts to orange with age. Increased vegetation cover appears yellow-green. This agrees with earlier TIMS results, and laboratory spectral studies.

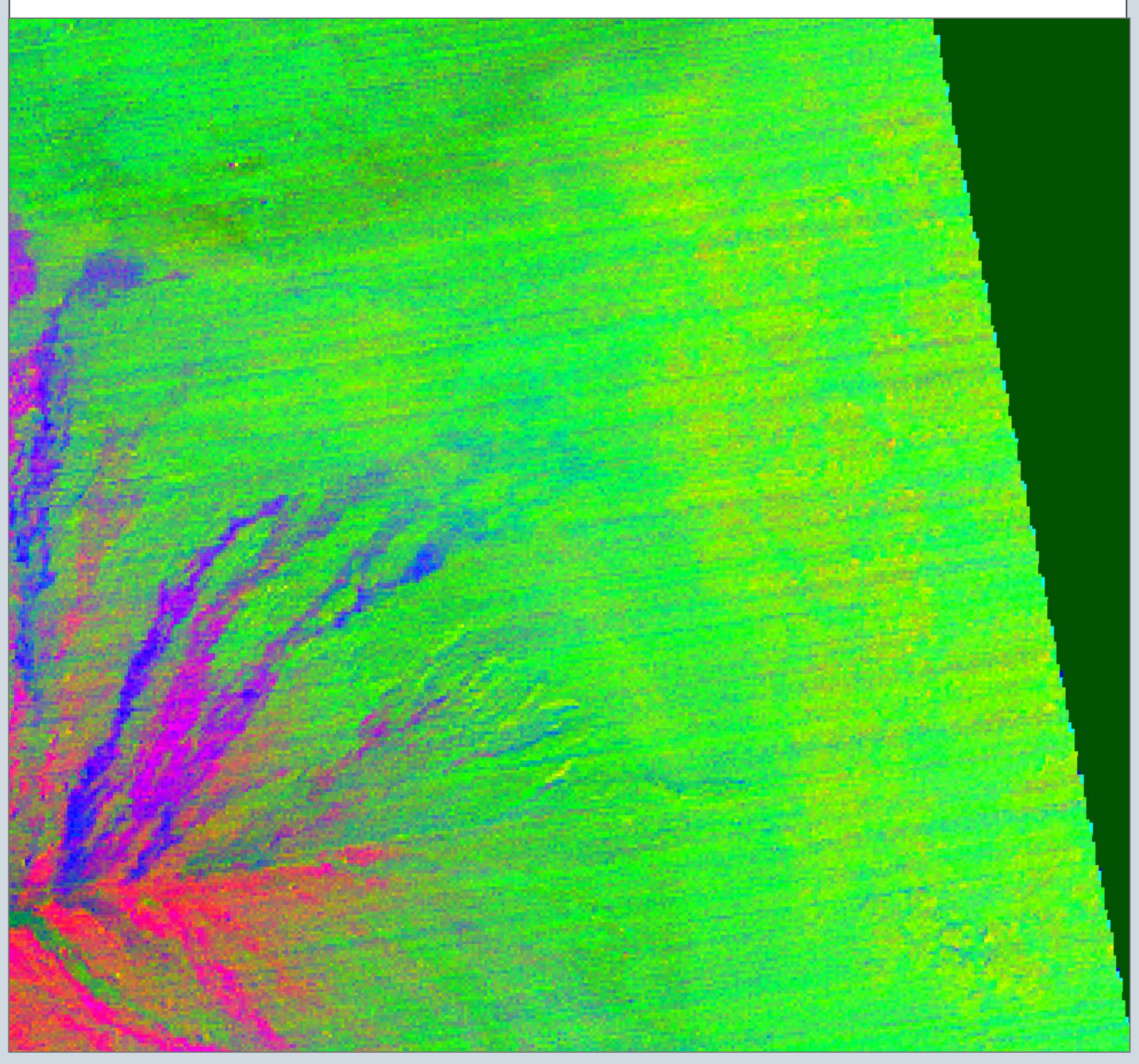

Fig. 4. Decorrelation stretch of nighttime ASTER image, bands 13-12-10 in RGB.

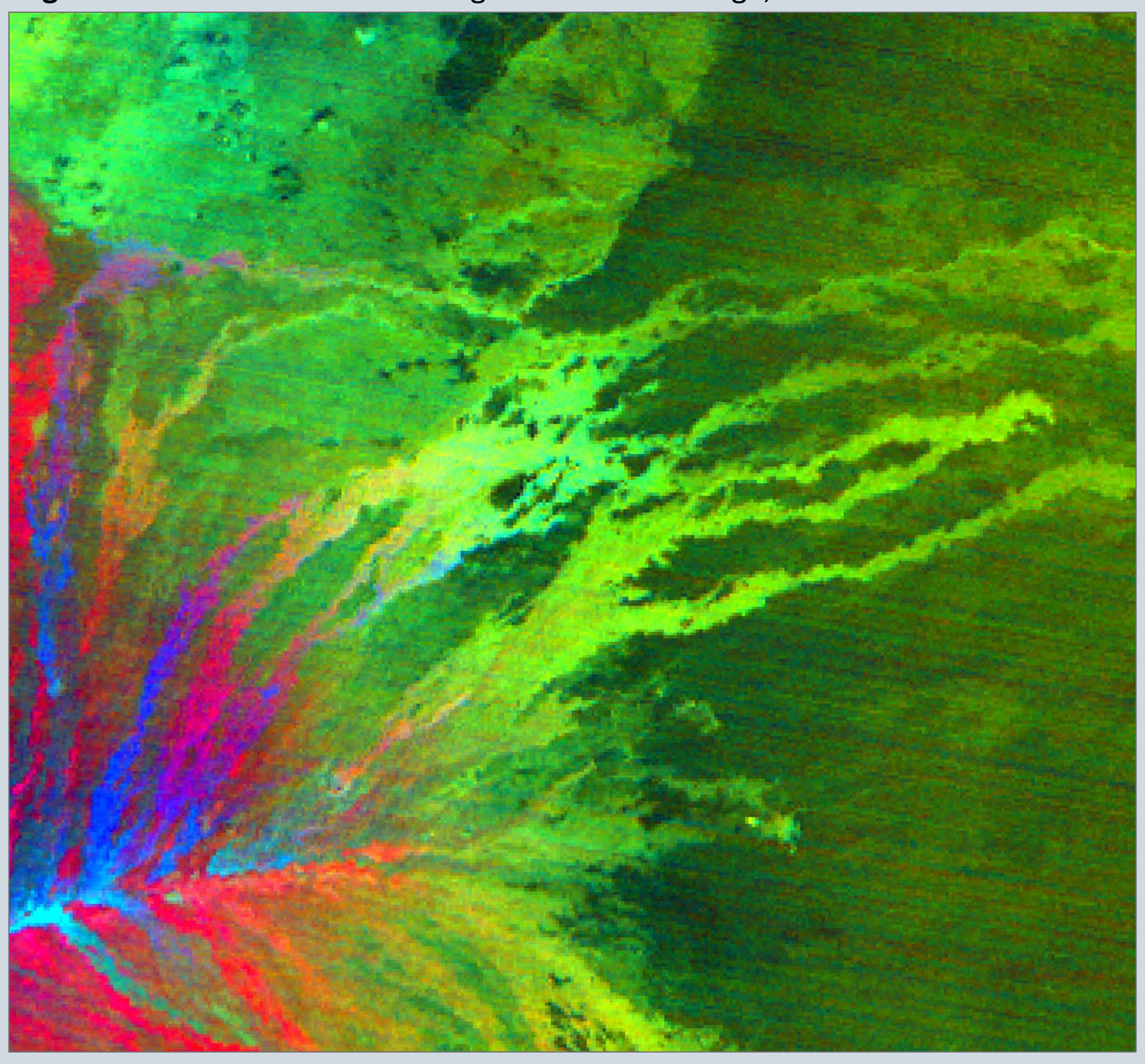

Fig. 5. Decorrelation stretch of daytime ASTER image, bands 13-12-10 in RGB.

We observe that the colors of the lava flows are consistent between the day and night ASTER images. The decorrelation stretch enhances emissivity variations and displays them as color variations, while showing temperature variations as brightness. As expected, the emissivity differences (colors) are invariant between the day and night data. In the day data, the flows in the northeast vegetated part of the image are separable from the background due to their higher temperature (brightness). Their color (green) is the same as the highly vegetated background, indicating that spectrally, the vegetation cover is the dominant influence.

We displayed nighttime ECOSTRESS bands 4, 3 and 1 in RGB and applied a decorrelation stretch (***Figure 6*** nighttime), using the same processing as applied to the ASTER data.

Comparing the two nighttime images, we see a close similarity in the colors of the different lava flows. The downslope, vegetated part of the ECOSTRESS image suggests that some of the younger flows are just visible against the heavily vegetated background.

The two data sets appear to have different levels of noise. The NEΔT of the instruments is 0.3 K for ASTER, and about 0.14 K for ECOSTRESS. Striping goes in different directions, but in both data sets, there is obvious evidence of residual miscalibration between detectors. The difference in spatial resolution (90 m for ASTER, and 70 m (re-sampled) for ECOSTRESS) is perhaps apparent in the data, augmented by the better NEΔT of ECOSTRESS. Visually, ECOSTRSS data appear sharper. The separation of vegetated lava flows from background also supports the improvement of ECOSTRESS over ASTER.

Several characteristics of ECOSTRESS emphasize its inherent operational advantage over ASTER. The significant difference in swath width (384 versus 60 kilometers) bestows two advantages: the larger area coverage means that significant parts of entire volcanic provinces can be imaged at one time. The Island of Hawaii is a good example at the lower spatial size. ASTER cannot image the entire island in one orbit. ECOSTRESS obviously can. But even more significant is the repeat coverage afforded by the larger swath width. We found 12 ECOSTRESS images of Hawaii in the six week period between August 2 and September 12. ASTER (if it had been targeting Hawaii) would have imaged the Mauna Loa area 3-4 times during the same period.

For dynamic phenomena, like volcanic eruptions with lava flows or eruption plumes, an ECOSTRESS-like instrument is the scanner of choice. NASA's recent Decadal Survey recommended the Surface Biology and Geology mission, with a wide-swath multispectral TIR scanner. ECOSTRESS can be seen as a pathfinder for SBG, supported by the past decade-long study for HyspIRI.

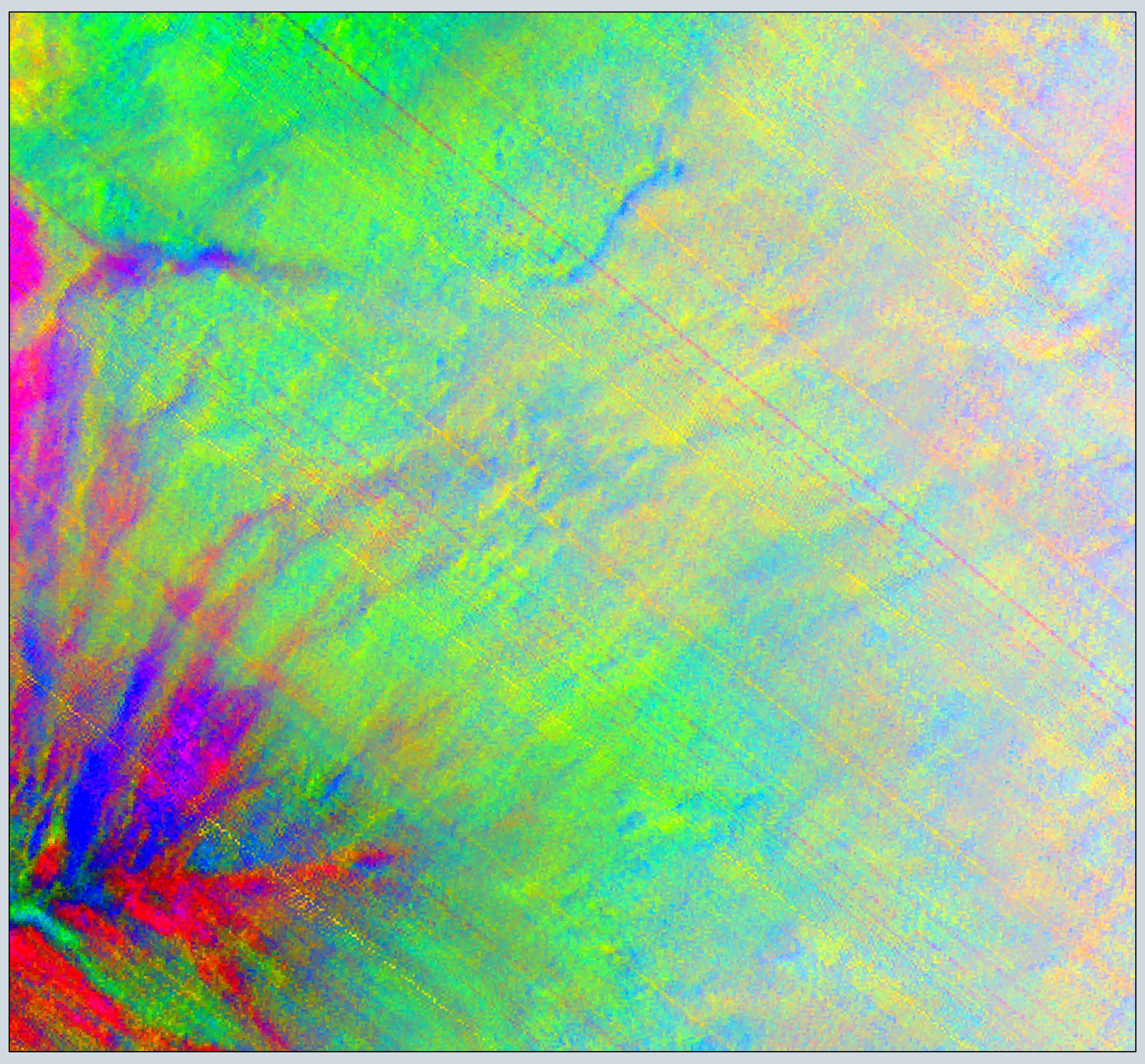

Fig 6. Decorrelation stretch of nighttime ECOSTRESS image, bands 4-3-1 in RGB.

Conclusions

ECOSTRESS and ASTER TIR data were compared for mapping lava flows on the northeast flank of Mauna Loa volcano, Island of Hawaii. ECOSTRESS bands 4-3-1 and ASTER bands 13-12-10 have almost the same wavelengths. Cloud-free nighttime ECOSTRESS and ASTER data were processed using decorrelation stretch to enhance emissivity features related to relative ages of the pahoehoe and a'a flows. The two data sets were closely comparable in information content. ECOSTRESS appears to have lower noise due to better NEΔT, and higher spatial resolution. ECOSTRESS has the advantage of 6X the swath width, and as a result, much more frequent repeat coverage. For active volcanoes, this is a major improvement over any other instrument currently in orbit.

Acknowledgement

This work was performed at the Jet Propulsion Laboratory, California Institute of Technology under contract with the National Aeronautics and Space Administration. Thanks to V. Realmuto and K. Cause-Nicholson (JPL) for help with data preprocessing and useful discussions.

References

E. Abbott, A. Gillespie, A. Kahle, "Thermal infrared imaging of weathering and alteration changes on the surfaces of basalt flows, Hawaii, *Int'l. J. Remote Sensing*, **34**, 3332-3355, 2013.

M. Abrams**,** E. Abbott, A. Kahle, "Combined use of visible, reflected and thermal infrared images for mapping Hawaiian lava flows", *J. Geophys. Res.*, **96**, 475-484A, 87-92, 1991.

J. Crisp, A. Kahle, E. Abbott, "Thermal infrared spectral character of Hawaiian basaltic glasses", *J. Geophys. Res.*, **95**, 21657-21669, 1990.

T. Farr and J. Adams, "Rock coatings in Hawaii*", Geol. Soc. Am. Bull.*, **95**, 1077-1083, 1984.

A. Kahle, A. Gillespie, E. Abbott, M. Abrams, R. Walker, G. Hoover, J. Lockwood, "Relative dating of Hawaiian lava flows using multispectral thermal infrared images: a new tool for geologic mapping of young volcanic terranes", *J. Geophys. Res.*, **93**, 15239-15251, 1988.

A. Trusdell and J. Lockwood, "Geologic map of the northeast flank of Mauna Loa volcano, Island of Hawai'i, Hawaii", *Scientific Investigations Map 2932–A*, pamphlet 25 p., 2 sheets, scale 1:50,000, https://doi.org/10.3133/sim2932A, 2017.